Nano-Structures & Nano-Objects 9 (2017) 26–30

Contents lists available at ScienceDirect

Nano-Structures & Nano-Objects

journal homepage: www.elsevier.com/locate/nanoso

Conditional optimisation of wet chemical synthesis for pioneered ZnO nanostructures

Debadrito Das [a], Animesh Kumar Datta [a,*], Divya Vishambhar Kumbhakar [a], Bapi Ghosh [a], Ankita Pramanik [a], Sudha Gupta [b]

[a] *Department of Botany, Cytogenetics, Genetics and Plant Breeding Section, University of Kalyani, Kalyani-741235, West Bengal, India*
[b] *Department of Botany, Pteridology and Palaeobotany Section, University of Kalyani, Kalyani-741235, West Bengal, India*

GRAPHICAL ABSTRACT

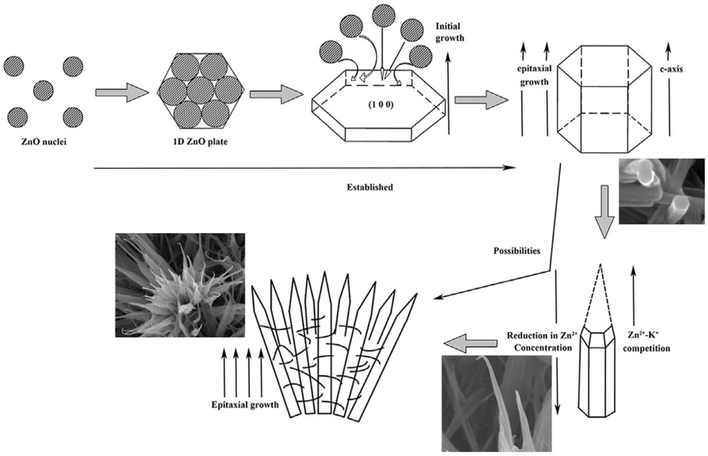

ARTICLE INFO

Article history:
Received 18 August 2016
Received in revised form
7 December 2016
Accepted 7 December 2016

Keywords:
ZnO nanostructures
Wet chemical synthesis
Conditional optimisation
Needle-topped nanorod
Nanorosette

ABSTRACT

A protocol for novel Zinc oxide nano-geometry has been developed through conditional (pH, solvent and temperature) optimisation of simple wet chemical based acidic route synthesis. A monodispersed needle-topped nanorod and nanorosette structures pioneered for technological devices are prepared. Possible reaction kinetics is proposed for the nanostructural growth. Prepared nanocrystals are opto-physically characterised using UV–visible spectroscopy, Fourier transform infra-red spectroscopy, X-ray diffraction, Dynamic light scattering-zeta potential and Field emission scanning electron microscopy.

1. Introduction

Semiconductor nanomaterials possessing unique opto-physical and electrical properties are the focus of applied nanoscale research for potential exploration in designing engineered devices [1,

---

[*] Corresponding author.
E-mail address: dattaanimesh@gmail.com (A.K. Datta).

http://dx.doi.org/10.1016/j.nanoso.2016.12.002

2]. Among them, class II–VI residing semiconducting nanostructures are the most studied type due to their wide application in fabricating electronic devices operational at shorter wavelength [3], production of transparent liquid crystal display electrodes [4], light emitting diodes [5], thin film transistors [6], microelectronic devices [7], among others. Zinc oxide (ZnO; a II–VI class compound having wide band-gap—3.37 eV and high exciton binding energy—60 meV) both in solitary and in doped form [8,9], is a promising material for technological advancement due to its opto-transparency [10,11], specialised conductivity [12], efficient electron mobility [13], room temperature luminescence near UV-region and piezo-electricity [14]. Precise regulation over size and shape of ZnO nano-morphology is the strong determining factor for efficient performance of integrated devices [15,16]. For the purpose, considerable importance has been projected upon formulation and fabrication of wide range nanoscale ZnO geometries including cuboid to spherical particles [11,17], rods [18–20], wires [12], needles [21], belts [22], pencils [23], disks [24], whiskers [25] and other characteristic shapes adopting different methods namely, chemical precipitation, thermal evaporation, chemical bath deposition, vapour-phase transportation, microwave assisted sol–gel modification and others. Among the different synthesis techniques, wet chemical co-precipitation is rather cost effective robust type preparation methodology without any need of complex instrumentation for the growth of NPs [26].

Present investigation is designed for the conditional optimisation of a novel ZnO nano-architecture by tuning the wet chemical aqueous reaction kinetics for engineered devices. Synthesised nanostructures are opto-physically characterised using UV–visible spectrophotometry (UV–Vis), Fourier transform infra-red spectrometry (FTIR), X-ray diffraction (XRD), Dynamic light scattering (DLS), Zeta potential and Field emission scanning electron microscopy (FESEM) for determination of nano-standard quality.

2. Materials and methods

2.1. Wet-chemical synthesis

Stock solutions of 0.01 M (pH 6.0) of Zinc acetate dihydrate [$(CH_3COO)_2Zn \cdot 2H_20$, AR-grade Merck-India], 0.01 M potassium nitrate (KNO_3, AR-grade, Merck-India) and 0.1 M (pH 12.8) sodium hydroxide (NaOH, AR-grade Merck-India) were prepared following the dilution of respective salts/pellets in deionised water. ZnO crystal precipitation reaction was carried out following acidic as well as basic route of wet chemical synthesis. Both reaction types were programmed under continuous stirring of the stock solution on a magnetic stirrer.

Low pH acidic route synthesis (AS) of ZnO-nanocrystals was performed under two experimental set-up conditions (AS-1 and AS-2). Growth and subsequent precipitation were obtained following drop wise micro-pipetting (20 μl/drop; 5 drops/min) of NaOH (4000 μl) into the stock acidic solution [AS-1: $Zn(CH_3COO)_2 \cdot 2H_2O:KNO_3$ :: 25 ml:25 ml; AS-2: $Zn(CH_3COO)_2 \cdot 2H_2O:KNO_3$ :: 30 ml:20 ml]. Final pH of the mixture was fixed at 6.2.

Basic route synthesis (BS) was carried out by drop wise (20 μl/drop; 5 drops/min) addition of $Zn(CH_3COO)_2 \cdot 2H_2O - KNO_3$(1:1) mixture (10 ml) into the 0.1 M NaOH stock (50 ml) under vigorous stirring. Final suspension was maintained at pH 11.6.

Under each experimental set-up, reaction temperature was kept at 30° ± 1 °C. Vigorous stirring of each resultant suspension was performed for 2 h.

2.2. Thermal deposition of ZnO-Nanostructure (NS)

For nano fabrication, ZnO-NS super saturated suspensions from each set (AS-1, AS-2 and BS) were drop-coated on silicon (Si)-wafer [(1 1 1) plane] (2 mm × 2 mm). Each wafer was subjected to place in muffle furnace (400 °C for 20 min, at the temperature ramp. rate of 50 °C–80 °C/min) for thermal deposition and planer typo of 1D ZnO-NS.

2.3. Characterisation

Opto-physical attributes of ZnO-NS (AS-1, AS-2 and BS) were studied following the use of UV–Vis, FTIR, XRD, DLS and Zeta analyser.

Absorbance efficiency near visible and infra-red spectrum region was analysed under UV–visible spectrometer (Perkin Elmer LAMBDA 1050) and Fourier transform infra-red spectrometer (Jasco FT/IR-6300) respectively. Structural and crystalline properties of synthesised NS powders were assessed by $\theta/2\theta$ X-ray diffractometer (Shimadzu LabX) using CuK_α radiation. Crystalline size (D_{nkl}) was estimated using Scherrer equation—$D_{nkl} = k\lambda/\beta\cos\theta$; where λ = wavelength of CuK_α radiation, β = full width and half maximum intensity, θ = diffraction angle of considered diffraction peak and k = shape factor constant. Average hydrodynamic diameter of the nanostructures was measured using dynamic light scattering analyser (Delsa^{TM} Nano C, Beckman Coulter). Zeta potential estimates the surface electric charge of the ZnO-NS as well as its morphological stability in the aqueous solution.

ZnO nanoarchitecture deposited was observed under Field emission scanning electron microscope (JOEL JSM-7600F).

3. Results and discussion

3.1. Optical and infra-red characterisation

UV–visible absorption plots of the studied NS samples demonstrate existence of broad peaks (Fig. 1(a)) in 350–390 nm (AS-1-370 nm; AS-2-395 nm; BS-376 nm) region corresponding to characteristic standard peak of hexagonal Wurtzite ZnO crystal [27], which is in well agreement with high purity of the sample types [28,29]. Particle sizing effect on the blue shifting pattern of the prepared nanosuspensions reveals decreasing size order as AS-2 > AS-1 > BS. Blue shift of absorption edge of AS-1 and AS-2 is possibly attributed to the resultant interparticle coupling effect as suggested earlier by Ramani et al. [30] rather than quantum confinement due to small size Bohr-excitation radius of ZnO [31]. Red shifting of absorption edge of BS nanosample indicates abundance of hexagonal nanorod formation [30], thereby mediating increase in intensity of optical absorption.

Composite IR plot of 3 studied ZnO nanocrystals (Fig. 1(b)) exhibits inverse peak at 3200–3600 cm^{-1} region corresponding to O–H vibration. Changes in peak morphology from intense sharp type (AS-1 and AS-2) to shallow broad type (BS) may be attributed to the variation in the crystal morphology coupled with trapped lattice water diversity. Transmissional peak shifting (BS: 508 cm^{-1}, AS-1: 493 cm^{-1} and AS-2: 466 cm^{-1}) of Zn–O bond vibration towards higher wave number is in proportionate with increase in pH potential of the suspension. Stretching vibration of NO_3 [32] in 800–1390 cm^{-1} region is recorded for both acidic route samples. Absence of such in BS sample indicates that the reaction mixture is devoid of NO_3 radical.

X-ray diffraction patterns of the synthesised ZnO-NS powders are illustrated in Fig. 1(c). XRD spectra of nanosamples reveal peak localisation within Bragg angles (2θ) between 20° and 80°. Comparative superposition of the scattered plots of the